Spectroscopy applied to observations of terrestrial light sources of uncertain origin

Karl D. Stephan,[a] Sagar Ghimire, and William A. Stapleton
Department of Technology and School of Engineering, Texas State University, San Marcos, Texas 78666

James Bunnell
29 Bounty Road W., Benbrook, Texas 76132-1003

(Received 1 September 2008; accepted 17 April 2009)

Sensitive spectroscopic instrumentation is now sufficiently portable to be used in field experiments involving terrestrial light sources as well as for astronomical observations. We report the results of a 20 night investigation of a phenomenon known as "Marfa lights" with the aid of a Schmidt-Cassegrain telescope and a CCD-array spectrometer. We show that the combination of computer azimuth and altitude logging, video recording, and continuous spectroscopy provides enough data for unequivocal identification of false positives such as distant streetlamps, automotive headlamps, and fires. We demonstrate that spectroscopic analysis of atmospheric molecular oxygen absorption can be used to determine distances of continuum-spectrum sources with an accuracy of 6% or better for distances of 4 km or greater. We also used astronomical objects for both directional references and approximate estimation of the system noise level in terms of minimum usable light flux.
[DOI: 10.1119/1.3130609]

I. INTRODUCTION

The combination of a portable telescope and a sensitive, rugged CCD-array spectrometer is a powerful means of analyzing light from remote sources. Although the use of such instrumentation has been traditionally limited to astronomy, there are terrestrial light sources whose nature also merits investigation. One such source is the phenomenon known as "Marfa lights," named for the small West Texas town near which the lights are reported to appear.[1,2]

In documentation going back to the 1800s, hundreds of witnesses attest to seeing lights in or near Mitchell Flats, an area between Marfa and the larger nearby town of Alpine. These lights appear at times and places where no conventional explanation for light sources is known. The lights reportedly appear only between sunset and sunrise, move at varying speeds, can rise and fall, separate and merge, often vary in color and intensity, and can last up to several hours. Observers have obtained numerous photographs and few video recordings of the lights, but these records are of limited usefulness in a study of scientific claims concerning their nature.

The only publication on this subject addressed primarily to a scientific audience was a report of a two-night investigation done by the Society of Physics Students at the University of Texas at Dallas in 2005.[3] The students concluded that all the moving lights they observed could be explained as automotive headlights. One of us (Stephan) presented a paper at the Texas Section Spring 2006 meeting of the American Physical Society in which we discounted various exotic causes for the lights such as antimatter and tiny evaporating black holes.[4]

Because the existence of Marfa lights is contested, they are a good subject for an experimental study using modern portable spectroscopic instrumentation. We have not yet obtained enough data to reach an unequivocal conclusion about the nature of Marfa lights. In searches for new high-energy particles, observers often collect large amounts of data and remove false positives. If all the events turn out to be false positives, the existence of the unknown particle is not disproved. Instead, the most that can be claimed is that the experiment sets an upper bound on the frequency with which the particle might occur under the prevailing experimental conditions. We approached our observations of Marfa lights in this spirit.

We designed and executed a 20 night field experiment in May and June 2008 at the Marfa Light View Park, a facility erected by the Texas Department of Transportation on US Highway 90 between Marfa and Alpine for the convenience of observers. During this time, no objects were sighted that met the criteria of Marfa lights. We obtained spectra of dozens of objects, some of which could have been mistaken for lights of unknown origin by casual observers. In every case we witnessed, an examination of position, movement, and spectral data allowed us to explain the observation in terms of well-understood natural or artificial phenomena such as headlights or biomass fires. However, it would be premature to conclude from the results of this limited study that genuine Marfa lights do not occur.

We will first describe our setup and procedure, including the use of astronomical objects to ascertain both the position accuracy and the optical sensitivity of the system. Then we present a case study that shows that visible wavelength absorption bands due to molecular oxygen can be used to estimate the distance to an object emitting continuum radiation. We show that this technique produces distance estimates with an accuracy of 6% or better for distances of about 4 km or greater. We then present data on the estimated frequency of occurrence of Marfa lights and the resources required for further investigations.

II. SETUP AND PROCEDURE

Because Marfa lights vary in reported brightness down to an intensity comparable to that of the brighter stars, we designed our instrumentation to be capable of producing spectra with adequate signal-to-noise ratios from light sources equivalent in visible intensity to stars with a magnitude of 2 or brighter. Simultaneously with optical spectra, we obtained

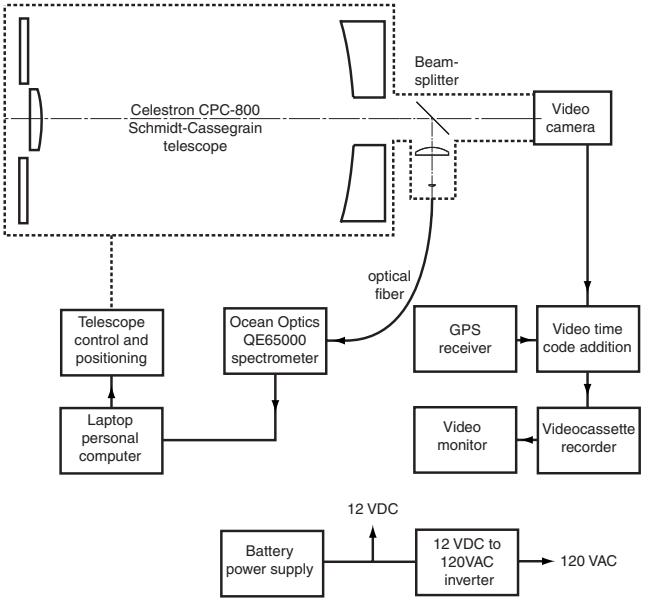

Fig. 1. Simplified diagram of telescope-camera-spectrometer setup.

a video image of the object to allow for manual tracking and video recording, with all data time stamped with the time data available from a GPS receiver. A simplified system diagram is shown in Fig. 1.

The telescope is a Celestron CPC-800 Schmidt-Cassegrain design with a 203 mm aperture. It was equipped with a 1-X finding sight and 8-X finding scope for initial sighting of objects of interest. We designed a splitter/imager system that was attached to the visual back of the telescope. The splitter/imager used a 75% reflectivity beam splitter mirror that directed most of the incoming light to two planoconvex lenses, which focused the beam onto a 1 mm diameter fiber-optic cable leading to an Ocean Optics QE65000 CCD-array spectrometer. This spectrometer uses a 1024 pixel CCD equipped with a 50 μm slit. This slit width produces a resolution of about 3 nm [full width at half maximum (FWHM)] when resolving a single atomic line. The size of the image produced by the splitter/imager on the fiber end was designed so that 50% or more of the peak on-axis optical power from a point source enters the fiber as long as the telescope is pointed to within ± 5 arc min of the source. Because the video camera used a 1/3 in. chip giving a field of view that was approximately 5×7.5 arc min, the fiber image size ensured that any luminous source visible through the camera could also produce a spectrum if its intensity was sufficient.

The camera was a low-light monochrome CCD unit (Super Circuits PC164C) designed for surveillance purposes, and fed analog NTSC video both to a monitor screen and to a videocassette recorder for logging. A GPS receiver connected to a video data-insertion device (KIWI OSD) produced a display on the monitor and VCR tape that showed the GMT time and serial number of each frame of the VCR recording. This arrangement allowed comparison of our data with other GPS-time-synchronized data.

The spectrometer and telescope were controlled and monitored with a notebook computer. All telescope control was manual, although a tracking feature could be added without much additional hardware. Custom software logged the azimuth and altitude data continuously from the telescope's motorized elevation-azimuth mount every 0.7 s. Although the telescope mount read out data with a resolution of less than 10 s of arc, gear backlash and other factors limit the true readout direction accuracy to about 0.08°–0.16°. The position data were also time stamped with GPS-synchronized time codes.

The spectrometer was set to capture a complete spectrum covering the 200–900 nm spectral range. A 10 s exposure provided adequate integration time for dim objects without saturating the CCD on bright objects. Accordingly, the spectrometer captured light from whatever was in the video monitor's field of view every 10 s during each night's observing period. To obtain a spectrum usable for absolute calibration and flux-intensity measurement, the object had to be exactly centered in the camera's field of view. We were able to center objects with this degree of precision only if they were either stationary or moving very slowly.

Power sources are one of the most important considerations in a field experiment where commercial power is not available. Two 17 AH (amp-hour) 12 V power packs using gel-type lead-acid batteries turned out to be inadequate, so they were supplemented with a 110 AH deep-discharge lead-acid battery, which we recharged during the day. This combination allowed continuous operation of the setup for at least 5 h. Operations generally commenced around the time of local sunset (between 8:30 and 8:45 p.m. CDT) and continued until midnight. Because the setup could not be left in place at the Marfa Light View Shelter for the duration of the study, it had to be disassembled and transported offsite at the end of each observation session. Portability was therefore a prime consideration.

III. CALIBRATION

A. Azimuth and altitude

Ideally, the location of an observed object should be established in three dimensions with an accuracy that allows determination of its height above the local ground. Luminous objects within 1 or 2 m of the ground have a much higher likelihood of being anthropogenic (for example, vehicle lights or flashlights), and moving objects that are more than 3 or 4 m above the ground are almost certainly airborne, especially when the ruggedness of the West Texas terrain is taken into consideration.

Even if an observation provides azimuth data with respect to true north and altitude data with respect to the true horizon, this data allows location of the object only along a line radiating from the observing station. Although triangulation from a second station would provide distance data, limited resources did not permit this approach. Instead, we developed two independent distance-measurement methods that apply well to objects that emit continuous spectra and are likely to be confined to paved roads. The headlamps of motorized vehicles were the most commonly observed mobile light source, and the results of our two independent distance-measurement methods agree well for this type of source. Other moving light sources we saw, such as locomotive headlamps and fireflies, were easy to distinguish without the use of instrumentation.

On nights when weather conditions permitted observations of Polaris, we carefully centered it in the view screen to log its position data and obtain spectra. Every night we also observed a stationary light on a microwave relay tower and used it as our working direction reference because it was

always visible regardless of cloud cover. To obtain a measure of the system's directional accuracy, we first corrected the raw altitude and azimuth data by observing the images of both Polaris and the microwave tower light on a video screen calibrated in arc min. We then derived correction factors to be added to the raw coordinates for Polaris to force the measured Polaris coordinates to agree with the actual coordinates of Polaris at the time, obtained from STARRY NIGHT software.[5] (Because the telescope position and zero point of the coordinate circles changed each night, a different set of correction factors had to be used each night.) We used these correction factors to correct the raw coordinate data for the microwave tower light. A sample of six azimuth and elevation bearings taken on the microwave tower light taken during six separate nights showed an average measured azimuthal bearing of 229.211° with a standard deviation of 5.5 arc min. The measured elevation was −0.507° with a standard deviation of 10.1 arc min. The true azimuthal bearing from our observation point to the microwave tower, as determined from independent geographic information system (GIS) data and onsite GPS-referenced measurements of the tower location, was 229.2° ± 0.1°, so the azimuth data agree very well with the GIS data. Because the height of the tower light was not known, no independent data are available to compare with the altitude measurements. One possible reason that the altitude data's standard deviation is about twice that of the azimuth data (10.1 versus 5.5 arc min) is that atmospheric refraction effects operate primarily in a vertical plane and may cause deviations of a few arc min in the apparent altitude of the microwave tower light from one night to the next. These calibration checks indicate that the directional accuracy of the system for objects such as the microwave tower light near the horizon is 16.5 arc min in azimuth and 30.3 arc min in altitude (3 standard deviations) when calibrated with Polaris. At a distance of 10 km, these angular errors cause a horizontal distance error of about 50 m and a vertical error of about 90 m. This degree of accuracy was acceptable for identifying all the objects we studied.

B. Relative and absolute intensity

If properly calibrated with light sources of known absolute intensity, a telescope-spectrometer setup such as the one we used in these experiments is capable of measuring the absolute light flux received from an object in a given wavelength range. Because we had no such absolute calibration source available, we were unable to perform an absolute calibration meeting the standards of accuracy that prevail in astronomical photometry.[6] We were able to use our Polaris sightings to test the night-to-night repeatability of the system's intensity measurements and to estimate the intensity of the system's minimum detectable signal. These data will prove useful in future efforts at absolute calibration, which would require a ground-based primary standard-intensity source such as that employed by Tüg *et al.*[7] or a secondary standard calibrated against such a primary source.

The first step in astronomical photometry involves obtaining the instrumental magnitude of the object whose absolute intensity is desired. If A is a measure of the total light flux from the object in a designated wavelength range, the instrumental magnitude m_I is defined to be

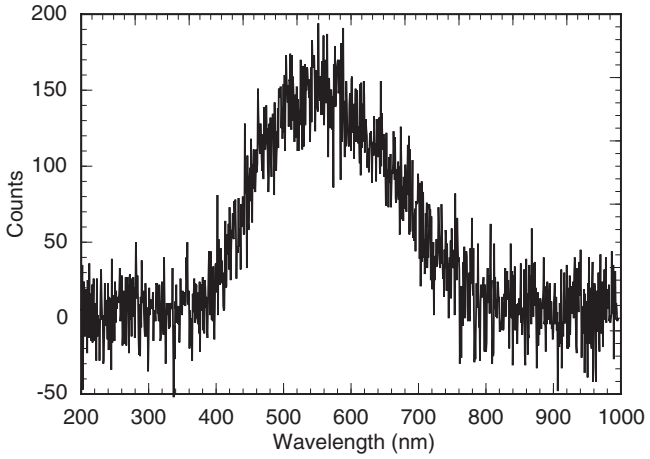

Fig. 2. Spectrum of Polaris taken on 3 June 2008 (after dark spectrum subtracted from the raw data).

$$m_I = -2.5 \log_{10}(A). \tag{1}$$

The negative sign occurs because brighter stars have lower (positive) magnitudes than dimmer stars.

Because the value of A depends on the wavelength range chosen, magnitudes are always stated with respect to a particular wavelength range. The commonly available tables of star's magnitudes are often expressed in terms of V, the star's magnitude in the visual wavelength band. The exact form of the V passband function is based on historical factors and is given in numerous sources, for example, Bessell.[8] This function peaks around 540 nm and has a FWHM of about 100 nm. To simplify our calculations, we approximated the V passband as a rectangular window whose value is unity from 500 to 590 nm and 0 otherwise.

To reduce the raw spectrometer readings for Polaris to instrumental magnitudes, we first subtracted a dark spectrum taken shortly after each Polaris observation (during telescope slewing when the instrument was not focused on a particular object). This subtraction compensated for any spectrometer dark-current drift because power limitations prevented us from operating the spectrometer's CCD array in a cooled controlled-temperature mode, and dark current is a sensitive function of array temperature. An example of the spectrum of Polaris taken on June 3 and corrected for dark current is shown in Fig. 2. Although the signal-to-noise ratio is only about 6:1, such a spectrum would still be usable for many purposes such as discriminating between a continuum source such as a star or an incandescent lamp, and a line or band source such as excited gas molecules or atoms.

After subtraction of the dark spectra, we converted several of our Polaris spectra to instrumental magnitudes by setting A in Eq. (1) equal to the average spectrometer count per pixel in the 500–590 nm band. Six measurements of Polaris on six different observing nights yielded a mean instrumental magnitude of −5.37 with a standard deviation of 0.14. One observation on 29 May 2008 was dimmer by 0.74 magnitude and not included in the average. (Possibly some thin clouds were present that night which reduced the reading.) The consistency of the magnitude measurements of Polaris indicate that the system is stable enough to produce instrumental magnitude data that are repeatable to better than 0.2 magnitude despite the handicap of disassembly and reassembly every night.

A rough estimate of the minimum detectable light flux can be obtained from Fig. 2 and information about the magnitudes of Polaris and Vega, a star that was not observed but is used as a reference-magnitude star in astronomical photometry. The absolute calibration of Vega by Tüg *et al.*[7] yielded a value of 1013 photons cm^{-2} s^{-1} in a 0.1 nm band centered at 544 nm for their Flagstaff observatory's location. Because Vega's magnitude is about 0, we estimate that Polaris's flux with its visual magnitude of 2 is about $10^{-(2/2.5)}=0.16$ times Vega's flux, which would give about 160 photons cm^{-2} s^{-1} in a 0.1 nm band from Polaris. As we have seen from Fig. 2, the flux from Polaris observed at our site is near the minimum detectable signal level and produces a signal-to-noise ratio of about 6:1. Therefore, we conclude that we can be able to analyze any light source that produces a flux of at least ≈160 photons cm^{-2} s^{-1} in a 0.1 nm band at our observing site. Most objects of interest produced intensities well in excess of this value and allowed us to obtain spectra with good to excellent signal-to-noise ratios.

IV. DISTANCE MEASUREMENTS USING OXYGEN ABSORPTION BAND

Molecular oxygen has a spectroscopic absorption band in the 760 nm region due to the $b\ ^1\Sigma_g^+ - X\ ^3\Sigma_g^-$ transition between the ground state and an excited state. This band was first noted by Fraunhofer in the solar spectrum and is often referred to as the Fraunhofer *A* band.[9] Because the depth of the absorption "notch" caused by this band is a monotonically increasing function of the optical depth of the atmosphere between the source and the observer, it has been used for various remote-sensing purposes such as determining cloud heights from satellites.[10] We found that sufficient absorption occurs in this band over path lengths as short as 1 km to permit estimation of the source-to-observer distance of continuum sources.

Our distance-estimation algorithm is a two-step process. In the first step, we use experimental data points that lie outside absorption bands to obtain a cubic polynomial fit to a small portion of the underlying continuum spectrum. We then use this polynomial to transform our raw data into a transmission function τ_{expt} whose value outside the absorption bands is approximately unity. Using expressions and tables derived by Pierluissi and Tsai[10] for their model of atmospheric transmittance in the *A* band, we can use the variables of atmospheric pressure, temperature, and optical path length to obtain a predicted or model transmission function τ_{MOD}. Next, we adjust the optical path length used in the model transmission function τ_{MOD} until the root-mean-square error between the experimental and model transmission functions is minimized. The path length that gives the minimum root-mean-square error between the two functions is the estimated distance to the source. Our algorithm thus produces a reasonably accurate estimate of the optical path length, which converts directly to distance if the atmospheric conditions are known. Because we also took barometric pressure and temperature data during our observations, we were able to apply this algorithm with good results.

When a source was known to be located on a road, its location could often be established independently by means of GIS and azimuth data. In these cases we could compare the distance calculated by the atmospheric oxygen-band absorption and GIS-azimuth approaches. These two methods agree within ±1.4 km or better for the examples we discuss.

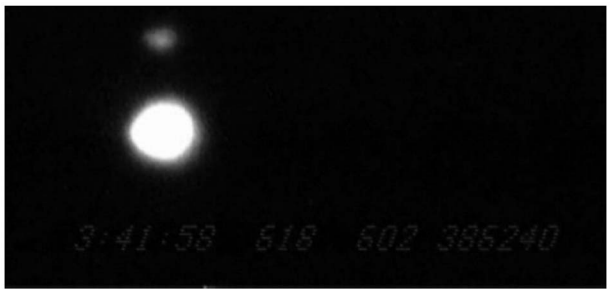

Fig. 3. Portion of video frame taken at 3:41:58 UTC 23 May 2008 (10:41:58 p.m. 22 May 2008 CDT), showing the appearance of a headlight pair at a distance of about 17 km during typical seeing conditions. Resolution into individual headlight images is impossible. The "ghost" image displaced upward from the large bright image is an artifact of the beam splitter system, and appears in all images of bright objects.

The Marfa Light View Park has a line-of-sight view of both Highway 90 (on which it is located) and portions of Highway 67, which runs south of Marfa toward the town of Presidio on the US-Mexico border. The most distant segment of Highway 67 that is visible from the park is about 38 km away. After the sun sets and most drivers have turned on their headlights, points of yellow-white light are easily seen over lines of sight this long. Atmospheric scintillation, which is always present to some extent, causes distortion and enlargement of the headlights as viewed either by the naked eye or through a telescope. Consequently, even with telescope optics the typical pair of headlights merges to present a blurry and changing outline which does not resemble headlights. Figure 3 is a portion of a video frame taken during 22 May 2008 and is a representative of the typical quality of "seeing" over paths of these lengths. Even though the source was relatively close (17 km), scintillation makes it impossible to resolve the image into two separate points of light. Note that due to internal reflections, the beam splitter optics superimpose a spurious "ghost" image of any bright object on the camera focal plane. This image was easy to recognize because it was always displaced a constant distance vertically above the true image. Because it was dimmer, the ghost image proved helpful in some instances when the main image was overexposed. The ghost image is clearly visible above the true image in Fig. 3.

On 28 May 2008, unusual atmospheric conditions produced a night of exceptionally good seeing. Figure 4 shows a

Fig. 4. Portion of video frame taken at 2:34:29 UTC 29 May 2008 (9:34:29 p.m. 28 May 2008 CDT) during period of exceptionally good "seeing" at a distance of about 31 km. Note that image of headlights to right is clearly resolved, especially in the less-exposed ghost image displaced vertically upward from the main image. The second pair of dots to upper left of headlights are tail lights of another vehicle receding to upper left.

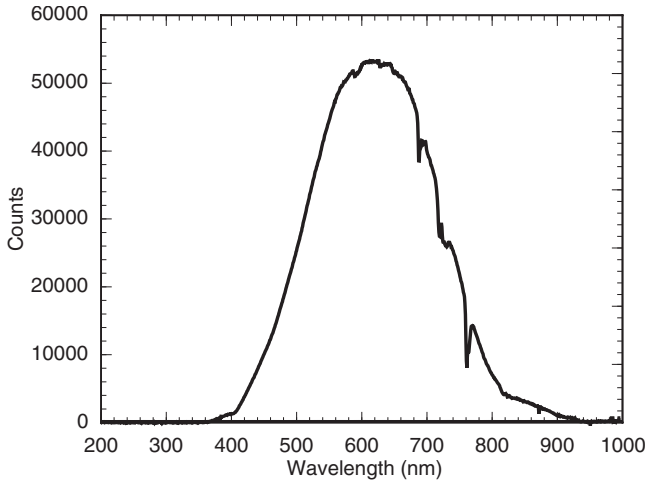

Fig. 5. Headlight spectrum obtained on 24 May 2008 and corrected only for zero offset. Note the molecular oxygen absorption bands at 690 and 760 nm.

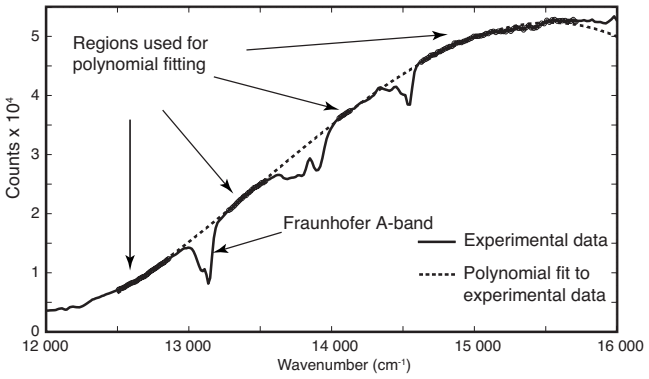

Fig. 6. Corrected experimental data (solid line) for the 24 May 2008 spectrum taken on 21:20:35 CDT, together with the cubic polynomial (dashed line) used to convert data to experimental transmission function τ_{expt}.

video frame of lights on two different vehicles about 31 km away from the observation point, nearly twice the distance of the headlights in Fig. 3. The separate headlights can now be resolved, especially in the less-exposed ghost image directly above the bright pair of dots in the lower right of the frame. The second pair of dots in the upper left is the true image of the taillights of a receding car going in the opposite direction to the headlights in the lower right. We encountered seeing of this quality on only one night out of 20. Fortunately, scintillation has little direct effect on the quality of visible light spectra, so even if the image of an unknown object scintillates badly, its spectrum is still usable.

The spectrum of a typical incandescent automotive headlamp is that of a tungsten-filament source at a temperature in the 2500–3000 K range. Over the wavelengths transmitted by the glass used in headlamps, the source is continuous and should show few if any narrowband features. However, during our initial field observations we noted that all headlight spectra showed absorption bands. Figure 5 shows a raw spectrum taken on 24 May 2008 directly from the spectrometer and corrected only for a zero offset. It is a continuum spectrum except for several molecular absorption bands, the strongest of which are near 690 and 760 nm. We now describe in more detail how we used the 760 nm absorption band in our distance-measurement algorithm.

Because the exact shape of the underlying continuum spectrum varies from source to source, each spectrum must be analyzed independently. After correcting the raw data for dark current with a dark-spectrum reference and converting wavelengths to wavenumbers $k=1/(\text{wavelength } \lambda \text{ in centimeters})$, we use experimental spectral data points outside the absorption bands to derive a cubic polynomial $P(k)$ which fits the continuum spectrum (except for the absorption bands) over the limited wavelength range from 636.47 nm (15712 cm^{-1}) to 799.46 nm (12508 cm^{-1}). (The wavelength-to-wavenumber conversion is for convenience in performing calculations because the transmission model data of Pierluissi and Tsai uses wavenumbers.) The cubic polynomial is our model for the source spectrum as it would appear to our spectrometer without the absorption bands. Figure 6 shows a portion of the data in Fig. 5 replotted versus wavenumber, along with the cubic polynomial fit to the data outside the absorption bands. The data points used for the polynomial fit were selected manually to lie outside the absorption bands.

Next, we derived an experimental transmittance function $\tau_{expt}(k_i)$ for each of 32 wavenumbers ($i=1-32$) covering the 760 nm Fraunhofer *A* absorption band, specifically from 13267 to 12870 cm^{-1}. The 32 data points correspond to the 32 pixels provided by the QE65000 spectrometer output over this selected width. The average resolution of the spectrometer is about 3 nm and the pixels are spaced about 0.75 nm apart in this region. If the raw spectrometer data in counts per wavenumber pixel (corrected only for the dark-spectrum background) are designated as $D(k_i)$, then the experimental transmittance function is

$$\tau_{expt}(k_i) = \frac{D(k_i)}{P(k_i)}, \tag{2}$$

where $i=1-32$. Equation (2) normalizes the experimental function $\tau_{expt}(k_i)$ so that its maximum value is approximately unity outside the absorption bands.

Pierluissi and Tsai[10] published tables and equations for the Fraunhofer *A* absorption band based on least-squares fits to experimental data. Their model allows one to calculate an expected model transmission function τ_{MOD} given the values of several variables, the most important of which are the wavenumber k (cm^{-1}) and the optical path length d (m). The model function also includes a dependence on air pressure and temperature, so we used our meteorological observations of these quantities to derive each model transmission function for a particular case. We calculated $\tau_{MOD}(k,d)$ in increments of 0.1 km (or 0.01 km for some of the shorter distances) over the appropriate range (typically from 1 km or less to 100 km), and for the 32 wavenumbers interpolated from the measured data. Finally, we plotted the root-mean-square error between the experimental and model transmission functions as a function of distance d,

$$\varepsilon(d) = \left[\frac{\Sigma_{i=1}^{N}(\tau_{expt}(k_i,d) - \tau_{MOD}(k_i,d))^2}{N}\right]^{1/2}, \tag{3}$$

which shows a smooth minimum at the distance that minimizes the error between the modeled and experimental transmission functions (see Fig. 7). The distance that minimizes this error is our best estimate of the distance involved. Figure 8 shows a comparison of the data-derived transmission func-

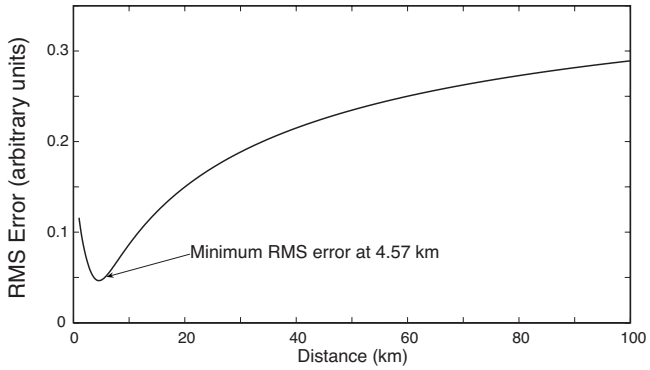

Fig. 7. RMS error $\varepsilon(d)$ in Eq. (3) as a function of the distance d for an observation of headlights on 24 May 2008 at 21:20:35 CDT. The minimum occurs at d=4.57 km.

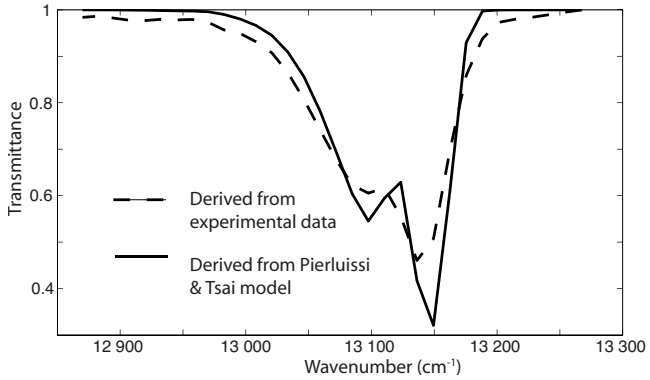

Fig. 8. Comparison of the transmission function derived from experimental data (dashed line) and the model transmission function of Pierluissi and Tsai (Ref. 10) for d=4.57 km.

tion and the Pierluissi and Tsai model function which corresponds to the minimum-error distance of 4.57 km shown in Fig. 7. Although this algorithm requires considerable effort, attempts to use simpler methods, such as measuring only the single minimum data point in the A-band curve or its width between fixed levels, failed to produce accurate results.

To check the accuracy of this method we used sightings of headlights in which the source's location was known from GIS data. The distance to vehicles on US Highway 67 can usually be determined within $\pm$0.5 km or better if the true bearing from the Marfa Light View Park is known, because the vehicle is located at the intersection of a bearing line and the two-lane highway. Such independent GIS distance measurements were made for six observations at GIS-calculated distances varying from less than 1–35 km, and compared with the distances estimated from our absorption-band algorithm. The results are shown in Table I.

As expected, longer distances lead to deeper absorption bands and greater accuracy. The observation at the greatest distance in Table I (35.65 km according to the GIS method) was taken on 14 May 2008, and the distance for that observation as measured with the absorption algorithm agrees with the GIS distance within 4%. The agreement is within 6% or better for distances in the 4 km range. Absorption is so small at a distance of less than 1 km (for example, the 26 May 2008 observation) that the distance error is on the order of the actual distance, but in absolute terms the absorption algorithm is still only 0.25 km in error compared to the GIS distance. An object this close can probably be located by other means, such as the use of elevation data and background scenery, so the absorption algorithm is useful mainly for distances exceeding 1 km.

We have shown that the 760 nm oxygen absorption band can be used to estimate distances of light sources with continuum spectra that include this band. When this approach is compared to independent distance measurements using GIS data, the agreement is 6% or better for distances greater than about 3–4 km.

V. DIRECT SPECTRAL IDENTIFICATION OF SOURCES

The direct identification of the type of light source from its observed spectrum is often straightforward. The easiest sources to identify are fixed streetlamps or exterior vapor lamps containing mercury or sodium because these elements have characteristic emission lines which are easily discerned. High pressure sodium lamps show significant pressure broadening and self-absorption, which allows for discrimination between high and low pressure sodium lamps.

A less well-known type of emission was observed twice during our stay. On the night of 16 May 2008 we observed a flickering stationary yellowish light south of the observing station and obtained its spectrum. Telescopic investigation showed a large irregular light source near some remote ranch buildings, suggestive of a bonfire or burning brush. On 4 June 2008 extensive grass fires took place north of our station, and we also obtained spectra of them. As Fig. 9 shows, both spectra reveal an intense double peak in the 767–770

Table I. Comparison of headlight distances measured by oxygen absorption band and GIS location.

Date (CDT)	Time (CDT)	True Azimuth (deg)	Distance Z_S (km) computed from 760 nm absorption spectrum	Distance Z_G (km) computed from azimuth and GIS data	Difference $Z_S - Z_A$ (km)
14 May	21:42:23	230.6	34.3	35.65	−1.35
22 May	23:39:54	256.0	35.7	34.42	1.28
24 May	21:20:35	97.6	4.57	4.73	−0.16
24 May	21:28:55	96.3	4.1	4.36	−0.26
24 May	21:30:35	96.3	4.1	4.36	−0.26
26 May	22:50:39	288.9	0.46	0.21	0.25

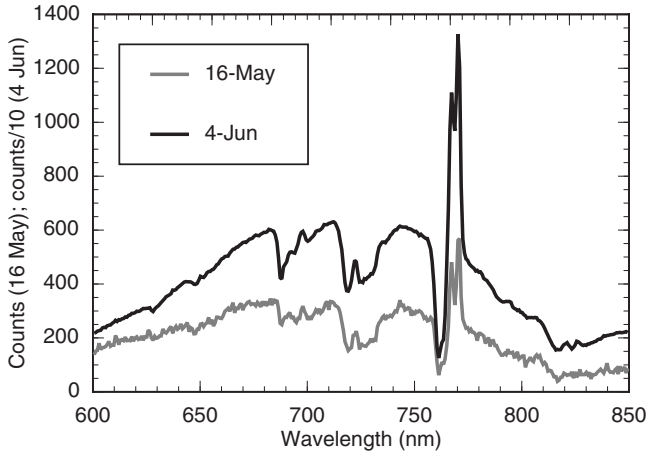

Fig. 9. Spectra of biomass fires observed on 16 May and 4 June 2008 (4 June data is multiplied by 0.1 for plot). Note prominent double-peaked potassium line at 767–770 nm.

nm in the near-IR region, in addition to the usual absorption bands we noted in other continuum sources. This double peak is due to potassium, and is commonly known to occur in biomass fires. Spectroscopy using this emission pair has been used to detect forest fires with orbiting satellites.[11]

VI. CONCLUSIONS AND RECOMMENDATIONS

Although we did not observe any objects during our 20 night stay that met the criteria for genuine Marfa lights, we showed that the combination of a portable telescope and CCD-array spectrometer can yield enough data to allow us to draw unequivocal conclusions on the origin of all light sources that were bright enough to produce spectra with an adequate signal-to-noise ratio. Stellar positions and intensities were used to calibrate the altitude, azimuth, and approximate sensitivity of the system for the visual band (500–590 nm), and we used the depth of the Fraunhofer *A* band due to atmospheric oxygen to determine the distance of several continuum sources. The accuracy of this type of distance measurement was verified with GIS distance data.

One of us (Bunnell) has maintained a set of unmanned observation stations using low-light video cameras trained on various portions of Mitchell Flats for several years.[12] These units are typically aimed away from frequently traveled roads to avoid false positives, and so may not capture all events of interest. This system of unmanned cameras proved useful for high-altitude atmospheric research when it captured images of the first gigantic jet ever recorded over continental North America.[13] (A gigantic jet is a high-altitude atmospheric phenomenon associated with thunderstorms.) Recovery and inspection of these digital recordings, which cover most nights during 2000–2008, have yielded numerous images whose motion and estimated intensity meet the criteria of genuine Marfa lights. These criteria include erratic off and on periods, gradual and sudden brightening, dimming, and eccentric motion not characteristic of automotive headlights, location in regions difficult to access by vehicle, splitting, merging, and other motion- and duration-related factors. Although spectral information is not currently obtainable from these monochrome camera data, these records are useful for making estimates of the phenomenon's frequency of occurrence. An analysis of these data shows that between November 2000 and May 2008, about 40 incidents were recorded that apparently fit the criteria for genuine Marfa lights. Because the incidents tend to occur in clusters (for example, several in a single night), the number of nights in which such objects were recorded was only 25, which is about 0.9% of the total number of nights monitored with the camera system. We conclude that a much more extended effort will be required to be reasonably certain of obtaining a spectrum of an object that meets the reported characteristics of genuine Marfa lights. These statistics help explain why our results during our 20 night stay are understandable in terms of the known phenomena and will serve as a guide for future efforts in this area.

ACKNOWLEDGMENTS

The authors acknowledge the support of V. Sriraman, Chair of the Texas State University Department of Technology, for providing personnel and equipment funds for this research. They also thank Irwin Wieder for helpful discussions, and Pamela Stephan and Benjamin Simons for much needed logistical help.

[a]Present address: Department of Technology, Texas State University, San Marcos, TX 78666. Electronic mail: kdstephan@txstate.edu

[1] Judith M. Brueske, *The Marfa Lights* (Ocotillo Enterprises, Alpine, TX, 1989).
[2] James Bunnell, *Night Orbs* (Lacey, Cedar Creek, TX, 2003).
[3] A. Stolyarov, J. Klenzig, P. Roddy, and R. A. Heelis, "An experimental analysis of the Marfa lights" <www.spsnational.org/wormhole/utd_sps_report.pdf>.
[4] K. D. Stephan, "What Marfa lights probably aren't," in *Texas Section Meeting of the American Physical Society*, San Angelo, TX, 24 March 2006 (abstract only available at http://meetings.aps.org/Meeting/TSS06/Event/50304).
[5] STARRY NIGHT, Complete Space and Astronomy Pack, Version 5.7.1 kcEM, manufactured by Imaginova Inc. (www.imaginova.com), 470 Park Ave. S., 9th Floor, New York, NY 10016.
[6] For a good description of the procedures needed for high accuracy astronomical photometry, *Handbook of CCD Astronomy*, 2nd ed. (Cambridge U.P., Cambridge, 2006).
[7] H. Tüg, N. M. White, and G. W. Lockwood, "Absolute energy distributions of α Lyrae and 109 Virginis from 3295 Å to 9040 Å," Astron. Astrophys. **61**, 679–684 (1977).
[8] M. S. Bessell, "UBVRI passbands," Publ. Astron. Soc. Pac. **102**, 1181–1199 (1990).
[9] P. Mardin, *Encyclopedia of Astronomy and Astrophysics* (Institute of Physics Publishing, Bristol, England, 2001), Vol. 1, p. 815.
[10] J. H. Pierluissi and C.-M. Tsai, "Molecular transmittance band model for oxygen in the visible," Appl. Opt. **25**, 2458–2460 (1986).
[11] A. Vodacek, R. L. Kremens, A. J. Fordham, S. C. Vangorden, D. Luisi, J. R. Schott, and D. J. Latham, "Remote optical detection of biomass burning using a potassium emission signature," Int. J. Remote Sens. **23**, 2721–2726 (2002).
[12] More information on these unmanned monitoring systems is available at <www.nightorbs.net>.
[13] O. A. van der Velde, W. A. Lyons, T. E. Nelson, S. A. Cummer, J. Li, and J. Bunnell, "Analysis of the first gigantic jet recorded over continental North America," J. Geophysical Research D **112**, D20104 (9 pages), doi:10.1029/2007JD008575 (2007).